

Published in final edited form as:

Mol Psychiatry. 2011 February ; 16(2): 156–170. doi:10.1038/mp.2010.50.

Mechanisms for Acute Stress-Induced Enhancement of Glutamatergic Transmission and Working Memory

Eunice Y. Yuen¹, Wenhua Liu¹, Ilia N. Karatsoreos², Yong Ren¹, Jian Feng¹, Bruce S. McEwen², and Zhen Yan^{1,*}

¹ Department of Physiology and Biophysics, State University of New York at Buffalo, School of Medicine and Biomedical Sciences, Buffalo, NY 14214

² Laboratory of Neuroendocrinology, The Rockefeller University, New York, NY 10065

Abstract

Corticosteroid stress hormones have a strong impact on the function of prefrontal cortex (PFC), a central region controlling cognition and emotion, though the underlying mechanisms are elusive. We found that behavioral stressor or short-term corticosterone treatment *in vitro* induces a delayed and sustained potentiation of the synaptic response and surface expression of NMDARs and AMPARs in PFC pyramidal neurons via a mechanism depending on the induction of serum- and glucocorticoid-inducible kinase (SGK) and the activation of Rab4, which mediates receptor recycling between early endosomes and the plasma membrane. Working memory, a key function relying on glutamatergic transmission in PFC, is enhanced in acutely stressed animals via a SGK-dependent mechanism. These results suggest that acute stress, by activating glucocorticoid receptors (GRs), increases the trafficking and function of NMDARs and AMPARs via SGK/Rab4 signaling, which leads to the potentiated synaptic transmission, thereby facilitating cognitive processes mediated by the PFC.

Keywords

acute stress; corticosterone; NMDA receptors; AMPA receptors; SGK; Rab4; working memory

Introduction

It has long been recognized that stress hormones have both protective and damaging effects on the body.¹ Acute stress is important for adaptation and maintenance of homeostasis, while chronic stress can produce maladaptive changes that lead to cognitive and emotional disturbances.^{2,3} Adrenal corticosterone, the major stress hormone, operates through mineralocorticoid receptors (MRs) and glucocorticoid receptors (GRs),⁴ which are co-expressed abundantly in limbic regions.⁵ The high-affinity rapidly-activated MRs are implicated in the onset of stress responses, while the low-affinity progressively-activated GRs are involved in the termination of stress reactions. MRs and GRs can regulate the transcription of genes that are involved in controlling G-protein coupled receptors, ion channels and transporters, leading to changes in membrane properties.⁶

The brain regions that are primary targets of stress hormones include hippocampus (mediating certain types of learning and memory), amygdala (mediating fear responses), and prefrontal cortex (mediating working memory, executive function and extinction of

*Correspondence: Zhen Yan, Ph.D., Department of Physiology and Biophysics, State University of New York at Buffalo, 124 Sherman Hall, Buffalo, NY, 14214, USA. zhenyan@buffalo.edu.

learning). Morphological and physiological studies have found that stress induces neuroplasticity in these regions at different levels, including structural plasticity, such as plastic changes in spine and dendrite structures, and functional plasticity, such as changes in synaptic efficacy and neuronal excitability.^{3,6,7} Prefrontal cortex (PFC) undergoes significant development during adolescence, and there is evidence suggesting that the juvenile brain is more sensitive to stressors than the adult brain.⁸ Most of previous studies have focused on the structural remodeling and behavioral deficits in mature PFC by chronic stress.^{9,10} The action of acute stress and stress hormones on PFC synaptic function, particularly during the adolescent period, is largely unknown.

The PFC network is composed of two major cellular constituents, the glutamatergic pyramidal principal neurons and the GABAergic interneurons. Glutamatergic transmission that controls recurrent excitation within PFC networks is crucial for working memory,¹¹ suggesting that NMDARs and AMPARs are potential key targets of stress hormones involved in PFC-mediated cognitive processes. In agreement with this, we have found that acute behavioral stressors, via GR activation, induce a prolonged potentiation of NMDAR- and AMPAR-mediated synaptic currents in PFC pyramidal neurons and facilitate working memory performance in young rats.¹²

The question that remains to be answered is how acute stress and glucocorticoids can have the enhancing effects on PFC synaptic function and PFC-mediated behaviors. Increased membrane trafficking of NMDARs and AMPARs seems to be responsible for the acute stress-induced plasticity in PFC.¹² To determine how acute stress regulates glutamate receptor trafficking, we focused on the role of Serum- and Glucocorticoid-Inducible Kinase (SGK), a family of immediate early genes transcriptionally stimulated by stress hormones,¹³ and the Rab family small GTPases, which are involved in all stages of membrane traffic.¹⁴ Results gained from this study have revealed a potential molecular mechanism underlying the positive actions of acute stress in the PFC.

Materials and Methods

Animals and Drugs

See Supplementary Materials and Methods (SMM) for details.

Electrophysiological recording in slices

The whole-cell voltage-clamp recording technique was used to measure evoked synaptic currents in rat layer V medial PFC (mPFC) pyramidal neurons as previously described.¹² Recordings were performed from age-matched animals with or without stress exposure. Some of the initial experiments were performed without knowledge of the treatment that the animals had received. There were no differences in the results from blinded and non-blinded experiments and therefore results were combined (See SMM for details).

Whole-cell recordings in acutely dissociated and cultured neurons

The mPFC neurons acutely dissociated from prepubertal (25–28 days old) male SD rats or PFC cultures from E18 embryos were prepared as previously described.¹⁵ Cultures were maintained in Neurobasal with B27 supplement (Invitrogen), which gave rise to a low level (~0.5 nM) of corticosterone in the medium. Whole-cell recordings of ligand-gated ion channel currents used standard voltage-clamp techniques.¹⁵ See SMM for details.

Western Blot and Co-immunoprecipitation

See SMM for details.

Transfection and small interfering RNA

Small interfering RNA (siRNA) was used to suppress the expression of various proteins. Cultured PFC neurons were transfected with siRNA (20 nM) targeting Rab4, Rab5, Rab11 (all from Santa Cruz), SGK1, SGK2, or SGK3 (all from Santa Cruz), together with EGFP (0.2 ng/μl), using the Lipofectamine 2000 method (Invitrogen, San Diego, CA). Constitutively active SGK1 (S422D), SGK3 (S419D) and siRNA-resistant silent mutations of SGK1, SGK3 and Rab4 were constructed using the QuikChange Multi Site-Directed Mutagenesis kit (Stratagene). The sequences of silent mutants are: CTTTATGCGGCCGAAATA (SGK1), GCAAAGTCCTCCTCGCAA (SGK3) and CTATAACGCACCTACTAAT (Rab4). Mutated nucleotides are underlined. All constructs were verified by DNA sequencing. Two to three days after transfection, electrophysiological analysis was conducted in GFP-positive neurons.

Immunocytochemical staining

Cultured neurons were fixed in 4% paraformaldehyde in PBS for 30 min and permeabilized with 0.2% Triton X-100 for 5 min. After 1 hr of incubation with 5% bovine serum albumin to block non-specific staining, cultures were incubated with the primary antibody at 4°C overnight. Antibodies used include anti-SGK1, anti-SGK2, anti-SGK3 (all 1:200, abcam), anti-Rab4, anti-Rab5 and anti-Rab11 (all 1:500, Santa Cruz). Glutamate receptors on the cell surface were detected as what we described before (See SMM for details).¹⁵

Behavioral tests

To test working memory, the T-maze delayed alternation task¹² was used (See SMM for details).

Statistics

Statistical significance between groups subjected to different treatments was assessed using unpaired Student's *t*-tests or ANOVA with *post hoc* Tukey tests. Working memory tasks were tested with ANOVA for repeated measures (RM ANOVA).

Results

Acute behavioral stressor or *in vitro* corticosterone treatment produces a delayed and sustained potentiation of glutamatergic transmission in PFC pyramidal neurons via GR activation

To study the impact of acute stress on synaptic transmission, we examined synaptic strength by measuring input/output curves of evoked synaptic responses, such as NMDAR-EPSC, AMPAR-EPSC and GABA_A-IPSC, in PFC pyramidal neurons from animals exposed to stressful events. In the present studies, a 20-min forced-swim paradigm¹² was used as one of the stress procedures. As shown in Figure 1A and 1B, NMDAR- or AMPAR-mediated excitatory synaptic responses induced by a series of stimulus intensities were markedly potentiated in neurons from stressed animals (NMDA: $p < 0.001$, ANOVA; AMPA: $p < 0.001$, ANOVA). *Post-hoc* analysis revealed a significant increase at 1–4 hr or 24 hr post-stress, compared to non-stressed control groups (NMDA: 1–4 hr post-stress: 0.7–1.2 fold increase, 24 hr post-stress: 1.0–1.2 fold increase, $n = 20$; AMPA: 1–4 hr post-stress: 0.6–1.0 fold increase, 24 hr post-stress: 0.5–1.1 fold increase, $n = 18$; $p < 0.001$). Neurons from stressed animals examined at 5 days post-stress showed no significant difference from those of control animals (NMDA: < 0.05 fold increase, $n = 12$; AMPA: < 0.05 fold increase, $n = 7$; $p > 0.05$). In contrast, GABA_A-mediated inhibitory synaptic responses were unchanged by acute stress at all time points (1–4 hr, 24 hr, 5 days) examined (Figure 1C). Recordings of AMPAR- and NMDAR-mediated EPSCs in the same cells were also performed. As shown

in Supplemental Figure 1, acute stress significantly increased both NMDAR-EPSC and AMPAR-EPSC to a similar extent in PFC pyramidal neurons. By contrast, acute stress only enhanced AMPAR-EPSC, but not NMDAR-EPSC, in hippocampal CA1 pyramidal neurons, suggesting that stress hormones have region specific actions. Whole-cell ionic current recordings (Supplemental Figure 2) in acutely isolated PFC pyramidal neurons (pure postsynaptic preparations) show that animals exposed to forced-swim stress had a significantly increased NMDAR and AMPAR current density, which was abolished by injection (i.p.) of the GR antagonist RU486 (10 mg/kg). This suggests that the stress-induced enhancement of glutamatergic transmission likely occurs through GR-induced modification of postsynaptic NMDA and AMPA receptors in PFC pyramidal neurons.

Next, we examined whether *in vitro* treatment with stress hormones mimics the effect of behavioral stress on glutamatergic signaling. PFC slices were exposed to different stress hormones or receptor agonists for a short period of time, and examined 1–4 hr following treatment. To fully activate both low-affinity GRs and high-affinity MRs, we used the high concentration of 100 nM corticosterone, as used in other *in vitro* studies of the corticosteroid stress hormone effects.^{16,17} A significant main effect was found with compound applications (Figure 1D, $F_{7,96}=32.4$, $p<0.001$, ANOVA). *Post-hoc* analysis indicated that corticosterone treatment (100 nM, 20 min) significantly increased the amplitude of NMDAR-EPSC (control: 210 ± 15.8 pA, $n=11$; cort: 427 ± 23 pA, $n=12$; $p<0.001$), which was blocked by pretreatment (30 min) with the GR antagonist RU486 (20 μ M, 201.9 ± 20.4 pA, $n=15$, $p>0.05$), while RU486 itself did not affect the basal NMDAR-EPSC (186.2 ± 17.5 pA, $n=14$, $p>0.05$). The vehicle (DMSO) had no effect (180.8 ± 17.1 pA, $n=16$, $p>0.05$), but a significant enhancing effect was found with the specific GR agonist dexamethasone (100 nM, 20 min, 400 ± 23.8 pA, $n=16$; $p<0.001$). No enhancement was found with the MR agonist aldosterone (10 nM, 20 min, 139.1 ± 21.3 pA, $n=9$, $p>0.05$). *In vitro* treatment with corticotrophin releasing factor (CRF, 200 nM, 20 min) in PFC slices, which lack the hypothalamic-pituitary-adrenocortical (HPA) axis to produce corticosterone, failed to enhance NMDAR-EPSC (179 ± 12.3 pA, $n=12$, $p>0.05$), suggesting that the effect of acute stress *in vivo* is not mediated by CRF receptors.

We further examined the onset kinetics of the effect of corticosterone treatment. As shown in Figure 1E, after corticosterone treatment (100 nM, 20 min) of PFC slices, a significant main effect was found on NMDAR-EPSC ($F_{7,54}=33.7$, $p<0.001$, ANOVA) and AMPAR-EPSC ($F_{7,58}=13.2$, $p<0.001$, ANOVA). *Post-hoc* analysis indicated that no immediate effect was detected within 30 min, and the significant potentiation was only observed ~1 hr following corticosterone treatment (NMDA: control: 115.9 ± 6.2 pA, $n=12$; 1 hr: 236.5 ± 19.9 pA, $n=8$; 3 hr: 313.1 ± 26.4 pA, $n=7$; $p<0.001$; AMPA: control: 64.7 ± 16.6 pA, $n=12$; 1 hr: 113.9 ± 11.7 pA, $n=8$; 3 hr: 166.7 ± 27.9 pA, $n=7$; $p<0.001$). A more prolonged time course was examined in cultured PFC neurons. Whole-cell NMDAR or AMPAR current density was significantly potentiated at 4 hr and 24 hr after corticosterone (100 nM, 20 min) treatment (Figure 1F). Moreover, the amplitude of miniature EPSC (mEPSC), a response from quantal release of single glutamate vesicles, was significantly increased in PFC cultures at 4 hr or 24 hr after corticosterone treatment, while the mEPSC frequency was not altered by corticosterone treatment (Supplemental Figure 2). These results suggest that similar to acute stress, corticosterone treatment of PFC, via the activation of GRs, causes a delayed but long-lasting enhancement of NMDA and AMPA responses.

To determine whether the corticosterone-induced change of NMDA and AMPA responses is due to altered trafficking of NMDARs and AMPARs, we carried out a quantitative surface immunostaining assay to examine surface NMDAR and AMPAR clusters in PFC cultures.¹⁵ Cultured neurons were treated with corticosterone (100 nM) for 20 min. Twenty-four hours after washing off corticosterone, immunostaining was performed in nonpermeabilized

conditions. Surface NMDARs were detected with an antibody against GFP in neurons transfected with N-terminally EGFP-tagged NR2A and NR2B, because of the lack of good antibodies against the N-terminal (NT) region of NR2A or NR2B. Endogenous surface AMPARs were detected with an antibody against NT-GluR1. As shown in Figure 1G, in corticosterone-treated cultures, the fluorescent GFP-NR2A, GFP-NR2B and GluR1 surface clusters on dendrites were markedly increased. Quantitative analyses (Figure 1H) show that corticosterone treatment caused a significant increase (2–3 fold of control) in the cluster density (#clusters/50µm dendrite) of NR2A (control: 16.5 ± 1.7 , $n=12$, cort: 31.9 ± 5.4 , $n=12$; $p < 0.05$, t test), NR2B (control: 9.0 ± 1.2 , $n=12$, cort: 26.7 ± 4.2 , $n=12$; $p < 0.05$, t test) and GluR1 (control: 15.2 ± 2.5 , $n=12$, cort: 46.4 ± 4.4 , $n=12$; $p < 0.001$, t test). The cluster size was also significantly up-regulated by corticosterone treatment (NR2A: 1.8 ± 0.32 fold of control; $p < 0.05$, t test; NR2B: 2.2 ± 0.52 fold of control; $p < 0.05$, t test; GluR1: 2.8 ± 0.39 fold of control; $p < 0.001$, t test). Fluorescence intensity of NR2A was unchanged (1.3 ± 0.04 fold of control; $p > 0.05$, t test), but significantly increased with NR2B (1.5 ± 0.12 fold of control; $p < 0.05$, t test) or GluR1 (1.56 ± 0.2 fold of control; $p < 0.05$, t test). These results suggest that corticosterone treatment of PFC increases NMDAR and AMPAR clusters on the plasma membrane.

It is known that the trafficking of GluR1, GluR2/3, and GluR4 are regulated by different molecules in different states.¹⁸ Our previous surface biotinylation experiments show that the surface expression of both GluR1 and GluR2 are increased in PFC from acutely-stressed animals,¹² suggesting that corticosterone increases the number of GluR1/2 heteromeric channels at PFC neuronal membrane. Because the majority of surface GluR1 receptors are extrasynaptic,¹⁹ we also examined whether corticosterone alters AMPARs at synapses. Synaptic AMPAR clusters were measured by detecting GluR1 co-localized with the synaptic marker PSD-95. As shown in Figure 1I, corticosterone treatment (100 nM, 20 min) induced a significant increase of synaptic GluR1 (co-localized with PSD-95) cluster density (#clusters/50µm dendrite) in cultured PFC pyramidal neurons (control: 12.7 ± 1.4 , $n=11$; cort: 24.1 ± 1.9 , $n=13$; $p < 0.001$, t test). The total GluR1 or PSD-95 cluster intensity was not changed by corticosterone. These results suggest that corticosterone treatment of PFC increases AMPARs on the synaptic membrane.

The effect of acute stress on glutamatergic transmission depends on the activation of serum- and glucocorticoid-inducible kinase (SGK)

Next, we examined potential mechanisms underlying the effect of acute stress or corticosterone treatment on glutamatergic transmission in PFC. Since GR is a ligand-inducible nuclear transcription factor,⁴ we speculate that the effect of GR is dependent on gene transcription and protein synthesis. Consistently, pre-treatment with the transcription inhibitor (actinomycin D or puromycin) or translation inhibitor (anisomycin D) abolished the enhancing effect of corticosterone treatment on NMDAR-EPSC in PFC slices (Supplemental Figure 3).

The onset kinetics of the corticosterone effect (> 1 hr) suggests that it might require the activation of immediate early genes downstream of GR. One of the most likely candidates is the serum- and glucocorticoid-inducible kinase (SGK),¹³ which is composed of three isoforms, SGK1, SGK2 and SGK3. To assess the potential involvement of SGK, we first examined whether the expression level of SGK is up-regulated in stressed animals. As shown in Figure 2A and 2B, a significant main effect was found on SGK1 ($F_{3,16}=11.8$, $p < 0.001$, ANOVA) and SGK3 ($F_{3,17}=13.1$, $p < 0.001$, ANOVA). *Post-hoc* analysis indicated that the level of SGK1 and SGK3, but not SGK2, was progressively elevated in PFC slices examined at 1–2 hrs post-stress (SGK1: 1 hr: 2.9 ± 0.2 fold of control, 2 hr: 3.2 ± 0.1 fold of control; $p < 0.01$; SGK3: 1 hr: 2.3 ± 0.2 fold of control, 2 hr: 3.3 ± 0.1 fold of control; $p < 0.01$). Note that the time course for the stress-induced up-regulation of SGK1/3 and the

potentiation of glutamatergic signaling is consistent. Moreover, the increase in SGK1/3 was blocked by i.p. injection with the GR antagonist RU486 (Figure 2C, 0.97–1.27 fold of control, $n=4$). RU486 itself did not affect SGK levels (0.92–0.97 fold of control, $n=4$).

SGK phosphorylates serine and threonine residues in the motif R-X-R-X-X(S/T).^{20,21} To further examine the role of SGK in corticosterone regulation of NMDARs and AMPARs, we pre-treated PFC neurons with a SGK substrate peptide (RPRAATF), which should competitively block the interaction of all SGK isoforms with their endogenous substrates. This peptide was coupled to the protein transduction domain of the human immunodeficiency virus (HIV) TAT protein (YGRKKRRQRRR), which rendered it cell-permeant.²² As shown in Figure 2D, application of TAT-SGK peptide (1 μ M) abolished the enhancing effect of corticosterone treatment (100 nM, 20 min) on NMDAR-EPSC (SGK peptide: 206.5 \pm 13.8 pA, $n=9$; SGK peptide+cort: 186.4 \pm 16.6 pA, $n=10$; $p>0.05$, t test), while a TAT-scrambled peptide (1 μ M) was ineffective (sc peptide: 191.6 \pm 10.5 pA, $n=10$; sc peptide+cort: 373.2 \pm 18.8 pA, $n=13$; $p<0.001$, t test). AMPAR-EPSC was also blocked by TAT-SGK peptide (Figure 2E, SGK peptide: 58.0 \pm 3.8 pA, $n=11$; SGK peptide+cort: 83.5 \pm 4.6 pA, $n=15$; $p>0.05$, t test), but not the TAT-scrambled peptide (Figure 2E, sc peptide: 77.2 \pm 6.6 pA, $n=13$; sc peptide+cort: 166.3 \pm 13.8 pA, $n=13$; $p<0.001$, t test).

Protein kinase B (PKB, also referred as Akt) is another kinase that has the similar substrate motif as SGK, R-X-R-X-X(S/T).²¹ To examine the potential involvement of PKB/Akt in corticosterone regulation of glutamatergic responses, we treated PFC slices with the specific Akt inhibitor, Triciribine (also known as Akt Inhibitor V), a cell-permeable tricyclic nucleoside that selectively inhibits the cellular phosphorylation/activation of Akt1/2/3 with little effect towards cellular signaling pathways mediated by SGK.²³ As shown in Figure 2D and 2E, pretreatment with Akt Inhibitor V (20 μ M, 30 min) failed to block the enhancing effect of corticosterone (100 nM, 20 min) on NMDAR-EPSC (Akt Inhibitor V: 150.5 \pm 16.4 pA, $n=8$; Akt Inhibitor V+cort: 357.0 \pm 31.5 pA, $n=11$; $p<0.001$, t test) and on AMPAR-EPSC (Akt Inhibitor V: 57.6 \pm 4.6 pA, $n=7$; Akt Inhibitor V+cort: 126.6 \pm 7.4 pA, $n=7$; $p<0.001$, t test). Moreover, no significant difference was found in the expression or activity of Akt (indicated by ^{Ser473}phosphorylated-Akt) in control vs. swim-stressed rats (data not shown). In addition to Akt, p42/44 MAPK has been shown to be involved in AMPAR trafficking during synaptic plasticity.^{24,25} However, pretreatment with the MAPK kinase inhibitor PD98059 (40 μ M, 30 min) did not block the enhancing effect of corticosterone (100 nM, 20 min) on AMPAR-EPSC (Figure 2E, PD98059: 66.8 \pm 6.4 pA, $n=8$; PD98059+cort: 128.9 \pm 9.8 pA, $n=7$; $p<0.001$, t test). These results rule out the involvement of PKB/Akt or p42/44 MAPK in the effect of corticosteroid stress hormones.

We also compared the acute stress-induced changes in glutamatergic transmission in PFC slices from animals with *in vivo* administration of TAT-SGK peptide. Previous studies have shown that intravenous (i.v.) injection can reliably deliver TAT peptides into CNS neurons,^{26,27} so we i.v. injected animals with TAT-SGK peptide at 30 min before the stress procedure. As shown in Figure 2F, forced-swim stress significantly increased the amplitude of NMDAR-EPSC in animals injected with the scrambled TAT-sc peptide (0.6 pmol/g, control: 174.1 \pm 11.8 pA, $n=16$; stressed: 383.0 \pm 25.2 pA, $n=15$; $p<0.001$, t test), but this effect was lost in animals injected with the TAT-SGK peptide (0.6 pmol/g, control: 174.6 \pm 13.9 pA, $n=15$; stressed: 156.4 \pm 13.5 pA, $n=19$; $p>0.05$, t test). Moreover, in animals injected with the scrambled TAT-sc peptide, forced-swim stress robustly increased mEPSC amplitude (Figure 2G, control: 12.7 \pm 0.7 pA, $n=7$; stressed: 19.6 \pm 1.7 pA, $n=11$; $p<0.001$, t test, Figure 2H), but not mEPSC frequency (control: 1.9 \pm 0.2 Hz, $n=6$; stressed: 2.2 \pm 0.4 Hz, $n=8$; $p>0.05$, t test). However, the effect of acute stress on mEPSC amplitude was lost in animals injected with TAT-SGK peptide (control: 12.6 \pm 0.3 pA, $n=8$; stressed: 12.7 \pm 0.7 pA,

n=8; $p>0.05$, t test). It suggests that the i.v. injected TAT-SGK peptide can indeed be delivered to PFC neurons and affect the action of behavioral stressor.

To identify which SGK is involved, we knocked down SGK isoforms in PFC cultures with siRNA transfection. As illustrated in Figure 3A, SGK1, SGK2 or SGK3 siRNA caused a specific and effective suppression of the expression of these kinases in GFP-positive neurons (see Supplemental Figure 4A for quantification). As shown in Figure 3B and 3C, corticosterone treatment (100 nM, 20 min) significantly increased NMDAR and AMPAR current density (pA/pF) in neurons transfected with a scrambled siRNA (NMDA: control: 20.4 ± 1.2 , n=10; cort: 47.5 ± 1.7 , n=15; $p<0.001$, t test; AMPA: control: 14.8 ± 1.1 , n=12; cort: 32.7 ± 1.6 , n=11; $p<0.001$, t test). This enhancing effect of corticosterone was lost in neurons transfected with SGK1 siRNA (NMDA: control: 18.8 ± 2.5 , n=10, cort: 19.9 ± 2.1 , n=11; AMPA: control: 15.5 ± 1.1 , n=10, cort: 16.2 ± 2.0 , n=10; $p>0.05$, t test) or SGK3 siRNA (NMDA: control: 22.7 ± 0.84 , n=10, cort: 17.2 ± 1.3 , n=15; AMPA: control: 16.8 ± 1.2 , n=9, cort: 15.4 ± 1.2 , n=12; $p>0.05$, t test), but was unaltered in neurons transfected with SGK2 siRNA (NMDA: control: 22.4 ± 1.6 , n=11, cort: 53.9 ± 4.6 , n=15; AMPA: control: 14.2 ± 1.1 , n=12, cort: 33.4 ± 2.4 , n=14; $p<0.001$, t test). Co-transfecting with the siRNA-resistant silent mutant of SGK1 (R SGK1) or SGK3 (R SGK3, Supplemental Figure 4C) rescued the enhancing effect of corticosterone (NMDA: R SGK1: control: 17.0 ± 1.0 , n=10; cort: 35.1 ± 1.9 , n=12; R SGK3: control: 14.7 ± 1.0 , n=8; cort: 30.9 ± 2.7 , n=7; $p<0.001$, t test; AMPA: R SGK1: control: 16.8 ± 1.1 , n=8; cort: 32.5 ± 1.9 , n=9; R SGK3: control: 16.3 ± 1.6 , n=9; cort: 29.6 ± 2.2 , n=8; $p<0.001$, t test), suggesting the specificity of these SGK siRNAs.

To confirm the role of SGK in corticosterone-induced changes in synaptic AMPAR responses, we measured mEPSC in SGK-knockdown neurons at 24 hrs after corticosterone treatment (100 nM, 20 min). As shown in Figure 3D and 3E, in neurons transfected with SGK1 siRNA, corticosterone lost the capability to increase mEPSC amplitude (control: 23.5 ± 1.5 pA, n=11; cort: 24.6 ± 1.2 pA, n=9; $p>0.05$, t test). However, the enhancing effect was intact in SGK2 siRNA-transfected neurons (control: 23.2 ± 1.5 pA, n=8; cort: 41.1 ± 2.5 pA, n=12; $p<0.01$, t test). To determine an imperative or permissive role of SGK, we further examined whether constitutively activating SGK (CA-SGK) occludes the corticosterone effect on mEPSC. As shown in Figure 3F and 3G, in neurons transfected with CA-SGK3, the basal mEPSC amplitude was significantly increased (GFP alone: 25.3 ± 1.3 pA, n=7; CA-SGK3: 35.5 ± 2.4 pA, n=8; $p<0.01$, t test), and corticosterone treatment had no further effect (33.2 ± 1.5 pA, n=9). The mEPSC frequency was not changed. Similar results were obtained from CA-SGK1 (data not shown). Taken together, these data suggest that the regulation of glutamatergic signaling by stress hormones requires the activation of SGK1/3 downstream of GRs.

The increase in Rab4-mediated receptor recycling underlies the enhancing effect of acute stress on glutamatergic signaling

The corticosterone-induced potentiation of NMDA and AMPA responses is accompanied by increased surface NMDAR and AMPAR clusters, suggesting that GR activation might influence the membrane trafficking of glutamate receptors. It is known that the Rab family of small GTPases functions as specific regulators of vesicle transport between organelles, and different Rab members control vesicular fusion at different stages in the exocytic/endocytic cycle.¹⁴ Among them, the most likely candidates are: Rab5, which controls the transport from plasma membrane to early endosomes,²⁸ Rab4, which controls a rapid direct recycling route from early endosomes to cell surface,^{29,30} and Rab11, which mediates recycling from recycling endosomes to plasma membrane.³¹

To test the potential involvement of Rab proteins, we examined the effect of corticosterone treatment on NMDAR and AMPAR currents in PFC cultures transfected with siRNA

against Rab4, Rab5 or Rab11. Immunostaining shown in Figure 4A verified the specific suppression of Rab4, Rab5 and Rab11 expression by these siRNAs in GFP-positive neurons (see Supplemental Figure 4B for quantification). As demonstrated in Figure 4B and 4C, knockdown of Rab4 blocked the increase of NMDAR or AMPAR current density (pA/pF) by corticosterone treatment (100 nM, 20 min) (NMDA: control: 19.9 ± 2.4 , $n=10$, cort: 16.4 ± 1.4 , $n=11$; AMPA: control: 17.3 ± 0.75 , $n=9$, cort: 16.3 ± 1.5 , $n=10$; $p > 0.05$, t test). Co-transfecting with the siRNA-resistant silent mutant of Rab4 (Supplemental Figure 4D) rescued the enhancing effect of corticosterone (NMDA: control: 14.1 ± 0.8 , $n=7$, cort: 27.8 ± 1.9 , $n=8$; AMPA: control: 17.4 ± 0.9 , $n=9$, cort: 28.9 ± 2.6 , $n=8$; $p < 0.001$, t test), suggesting the specificity of Rab4 siRNA. In contrast, the enhancing effect of corticosterone was not altered by Rab5 siRNA (NMDA: control: 14.9 ± 1.0 , $n=8$, cort: 36 ± 3.2 , $n=8$; AMPA: control: 15.9 ± 1.6 , $n=9$; cort: 29.9 ± 2.1 , $n=11$; $p < 0.001$, t test). Rab11 siRNA also failed to affect corticosterone-induced increase in NMDAR or AMPAR current density (NMDA: control: 12.6 ± 1.0 , $n=10$, cort: 28.6 ± 2.7 , $n=9$; AMPA: control: 13.2 ± 0.8 , $n=10$, cort: 26.8 ± 2.0 , $n=9$; $p < 0.001$, t test).

To confirm the role of Rab4 in corticosterone-induced AMPAR synaptic delivery, we measured mEPSC in Rab4-deficient neurons at 24 hrs after corticosterone treatment (100 nM, 20 min). As shown in Figure 4D and 4E, in neurons transfected with a scrambled siRNA, corticosterone significantly increased mEPSC amplitude (control: 27.1 ± 1.5 pA, $n=8$, cort: 43.4 ± 2.1 pA, $n=10$; $p < 0.001$, t test). In Rab4 siRNA-transfected neurons, the effect of corticosterone on mEPSC amplitude was lost (control: 27.0 ± 1.1 pA, $n=8$; cort: 27.8 ± 1.6 pA, $n=7$; $p > 0.05$, t test). In contrast, Rab5 siRNA-transfected neurons had an intact enhancing effect with corticosterone treatment on mEPSC amplitude (control: 24.9 ± 1.3 pA, $n=11$; cort: 38.5 ± 2.7 pA, $n=9$; $p < 0.001$, t test). These results suggest that the corticosterone-induced increase in functional glutamate receptors is through a mechanism depending on Rab4-mediated receptor recycling.

To further test the involvement of Rab4, we examined whether acute stress could increase the activity of this small GTPase. Since Rabaptin-5, a molecule originally identified as a Rab5-interacting protein, binds to only the GTP-bound, active form of Rab4 and Rab5 at its N- and C-terminus, respectively,³² we measured Rabaptin-5-bound Rab4 and Rab5 by co-immunoprecipitation experiments to indicate their activity levels. As shown in Figure 5A, corticosterone treatment (100 nM, 20 min) of PFC slices induced a significant increase of Rab4 activity, as indicated by the elevated level of Rabaptin-5-bound Rab4 (2.1 ± 0.16 fold of control, $n=4$; $p < 0.001$, t test), while it did not alter the Rabaptin-5-bound, active form of Rab5 (1.05 ± 0.11 fold of control, $n=4$; $p > 0.05$, t test). Pre-treatment of PFC slices with TAT-SGK peptide (50 μ M, 30 min) blocked corticosterone-induced elevation of Rab4 activity (1.25 ± 0.23 fold of control, $n=4$; $p > 0.05$, t test), suggesting the SGK dependence of this effect.

To determine whether acute behavioral stress also activates Rab4, we examined PFC slices from stressed animals. As shown in Figure 5B, the level of Rabaptin-5-bound, active Rab4 was significantly increased by acute stress ($F_{4,18}=10.7$, $p < 0.001$, ANOVA), which was observed at 0.5–2 hrs post-stress (1.55 ± 0.2 fold of control, $n=5$; $p < 0.01$, Tukey). In contrast, no difference was observed in the level of Rabaptin-5-bound, active Rab5 (1.02 ± 0.18 fold of control, $n=4$; $p > 0.05$). Taken together, these data suggest that acute stress selectively increases Rab4 activity in PFC via SGK signaling, which may facilitate the recycling of glutamate receptors to plasma membrane.

Next, we performed immunocytochemical studies to directly test the role of SGK in glutamate receptor trafficking. First, we measured the density of synaptic GluR1 clusters (co-localized with the synaptic marker PSD-95) in PFC cultures treated with TAT-SGK

peptide. As shown in Figure 5C and 5D, about 1 hour after corticosterone treatment (100 nM, 20 min), a significantly potentiated synaptic delivery of AMPARs was observed in neurons pretreated with the scrambled TAT-sc peptide (synaptic GluR1 clusters/50 μ m dendrite: control: 13.7 ± 1.4 , $n=12$, cort: 27.6 ± 2.4 , $n=11$; $p < 0.001$, t test), but not the TAT-SGK peptide (control: 13.3 ± 1.6 , $n=12$, cort: 16.0 ± 2.1 , $n=12$; $p > 0.05$, t test). These results suggest that corticosterone-induced delivery of glutamate receptors to the synaptic membrane requires SGK.

To directly test the role of Rab4 in AMPAR trafficking, we co-stained GluR1 and Rab4. As shown in Supplemental Figure 5, AMPA receptors could be seen in Rab4-positive internal vesicles. We also measured the impact of Rab4 knockdown on corticosterone-induced insertion of AMPARs. As shown in Figure 5E and 5F, in scrambled siRNA-transfected neurons, corticosterone treatment (100 nM, 20 min) significantly increased the surface GluR1 cluster density (#clusters/50 μ m dendrite) (control: 15.7 ± 1.4 , $n=22$; cort: 38.9 ± 2.2 , $n=26$; $p < 0.001$, t test), cluster size (μm^2) (control: 0.19 ± 0.02 ; cort: 0.34 ± 0.04 ; $p < 0.001$, t test), and fluorescence intensity (control: 132.5 ± 9.4 ; cort: 183 ± 16.9 ; $p < 0.05$, t test). However, in Rab4 siRNA-transfected neurons, the enhancing effect of corticosterone was blocked (cluster density: control: 12.9 ± 0.9 , $n=26$; cort: 16.9 ± 1.7 , $n=22$; cluster size: control: 0.14 ± 0.02 ; cort: 0.16 ± 0.02 , intensity: 125.6 ± 12.3 ; cort: 138.4 ± 12.9 ; $p > 0.05$, t test). These results suggest that Rab4 is required for corticosterone-induced potentiation of AMPAR membrane trafficking.

Our results suggest that acute stress simultaneously enhances the synaptic trafficking of NMDARs and AMPARs in PFC. It is possible that the potentiated AMPAR response is secondary to the potentiated NMDAR response, alternatively, the potentiated NMDAR response is secondary to the potentiated AMPAR response. To test this, we blocked the activation of one receptor and tested the effect of corticosterone on the other. As shown in Supplemental Figure 6, pretreatment with the NMDAR antagonist APV could not prevent corticosterone-induced increase in AMPAR-EPSC, and pretreatment with the AMPAR antagonist NBQX could not prevent corticosterone-induced increase in NMDAR-EPSC. It suggests that NMDARs and AMPARs are independently delivered to synapses by acute stress.

The acute stress-induced enhancement of working memory is linked to GR/SGK signaling

Since AMPAR- and NMDAR-mediated synaptic transmission at recurrent synapses in PFC networks is crucial for working memory,^{11,33} the acute stress-induced enhancement of glutamatergic responses could be linked to improved working memory (WM) in animals exposed to acute stress. Thus, we performed behavioral tests using the delayed alternation task in the T-maze, a well-established protocol for PFC-mediated WM.³⁴ To provide a “causal link” between stress-induced changes in glutamatergic transmission and WM, we tested whether TAT-SGK peptide, which blocked the effect of acute stress on glutamatergic transmission *in vitro*, could influence the effect of acute stress on WM.

First, animals were i.v. injected with TAT-SGK peptide (0.6 pmol/g) or a scrambled control peptide (TAT-sc, 0.6 pmol/g) at 30 min before the stress procedure, and the behavioral performance was examined at 4 hrs and 24 hrs post-stress. As shown in Figure 6A, forced-swim stress significantly increased WM performance at both time points ($F_{1,16}=32.2$, $p < 0.001$, RM ANOVA), and this enhancing effect was only observed in rats with the scrambled TAT-sc peptide administration (pre-test: $64.0 \pm 2.4\%$ correct, 4 hr post-stress: $75.0 \pm 3.2\%$ correct, 1 day post-stress: $83.0 \pm 2.7\%$ correct, $n=5$; $p < 0.01$), but not those with TAT-SGK peptide injection (pre-test: $63.0 \pm 3.2\%$ correct, 4 hr post-stress: $58.0 \pm 2.5\%$ correct, 1 day post-stress: $60.0 \pm 2.6\%$ correct, $n=5$; $p > 0.05$). Similarly, after exposure to elevated platform stress (Figure 6B), an improvement in WM was detected ($F_{1,20}=35.4$,

$p < 0.001$, RM ANOVA), only in rats injected with the scrambled TAT-sc peptide (pre-test: $62.3 \pm 1.8\%$ correct, 4 hr post-stress: $85.0 \pm 2.2\%$ correct, 1 day post-stress: $80.0 \pm 3.0\%$ correct, $n = 6$; $p < 0.01$), but not those injected with TAT-SGK peptide (pre-test: $63.0 \pm 3.0\%$ correct, 4 hr post-stress: $63.3 \pm 4.2\%$ correct, 1 day post-stress: $60.0 \pm 3.0\%$ correct, $n = 6$; $p > 0.05$). These results suggest that blocking SGK function abolished the enhancing effect of acute stress on WM.

To test the specificity of TAT-SGK peptide on PFC, we performed stereotaxic injection of the peptide to PFC prelimbic regions bilaterally via an implanted guide cannula. The scrambled TAT-sc peptide was locally injected as a control. A two-way RM ANOVA (Figure 6C) revealed significant effects of the peptide ($F_{3,32} = 46.34$, $p < 0.001$), the time of pre-/post-stress ($F_{2,32} = 18.83$, $p < 0.001$), and a peptide by time interaction ($F_{6,32} = 10.38$, $p < 0.001$). *Post-hoc* analysis revealed that the enhancing effect of elevated platform stress on working memory was unaffected by the scrambled TAT-sc peptide (40 pmol/g, pre-test: $62.0 \pm 2.0\%$ correct, 4 hr post-stress: $78.0 \pm 2.0\%$ correct, 1 day post-stress: $84.0 \pm 2.5\%$ correct, $n = 5$; $p < 0.01$). However, TAT-SGK peptide (40 pmol/g) blocked the stress facilitation effect completely (pre-test: $62.2 \pm 2.1\%$ correct, 4 hr post-stress: $64.0 \pm 2.4\%$ correct, 1 day post-stress: $60.0 \pm 1.0\%$ correct, $n = 6$; $p > 0.05$). Injection of a much lower dose of TAT-SGK peptide (0.12 pmol/g) to PFC produced a similar blockade (pre-test: $61.0 \pm 1.0\%$ correct, 4 hr post-stress: $60.0 \pm 2.0\%$ correct, 1 day post-stress: $58.5 \pm 2.4\%$ correct, $n = 5$; $p > 0.05$), while the same concentration of scrambled TAT-sc peptide failed to do so (pre-test: $60.0 \pm 1.0\%$ correct, 4 hr post-stress: $78.0 \pm 3.7\%$ correct, 1 day post-stress: $80.0 \pm 3.2\%$ correct, $n = 5$; $p < 0.01$). These data suggest that the acute stress-induced enhancement of working memory is causally linked to the GR/SGK-mediated enhancement of glutamatergic transmission within PFC.

Discussion

PFC is a key target region of stress,^{3,9,10} however the action of corticosteroid stress hormones on PFC synapses and the underlying mechanisms are largely unknown. In this study, we demonstrate that acute stress induces a long-lasting potentiation of glutamatergic transmission in PFC pyramidal neurons from young rodents, which is likely caused by the GR/SGK/Rab4-induced increase in the delivery of NMDARs and AMPARs to the synaptic membrane. Given the dependence of working memory on AMPAR- and NMDAR-mediated synaptic transmission in PFC recurrent synapses,^{11,33} the acute stress-induced enhancement of PFC glutamatergic transmission could directly impact on the activity of PFC circuits and therefore working memory performance.

Mounting evidence has indicated that corticosteroid hormones exert concentration- and time-dependent influence on hippocampal excitatory synaptic transmission and synaptic plasticity.^{6,35} An inverted-U relationship between the level of corticosterone and the magnitude of hippocampal long-term potentiation (LTP) was discovered in earlier studies.³⁶ Acute stress has also been found to facilitate long-term depression (LTD) and inhibit LTP³⁷ in hippocampus via a mechanism depending on GRs and protein/RNA synthesis.³⁸ Recent studies further revealed a rapid membrane MR-mediated increase of mEPSC frequency,³⁹ AMPAR surface diffusion¹⁷ and facilitation of synaptic potentiation,⁴⁰ as well as a slow intracellular GR-mediated increase of EPSC amplitude,¹⁶ AMPAR surface mobility and synaptic content¹⁷ and impairment of synaptic potentiation,⁴¹ in hippocampal neurons. Compared to these findings, our results have demonstrated several differences regarding the effect of acute stress and corticosterone in PFC. First, only the delayed, long-lasting GR-mediated postsynaptic effect was observed, which was probably due to the low abundance of MR expression in frontal cortex;⁶ Second, GR activation enhanced both AMPAR and NMDAR trafficking and function; Third, the GR-induced potentiation of glutamatergic

transmission in PFC might serve as a form of LTP induced by natural stimuli (e.g. stress), since PFC usually does not exhibit electrical stimulation-induced LTP.^{42,43} We found that pretreatment with the NMDAR antagonist APV could not prevent corticosterone-induced increase in AMPAR-EPSC, suggesting that the stress hormone-induced long-lasting potentiation of glutamatergic transmission in PFC is different from the activity-dependent, NMDAR-dependent LTP in hippocampus.

The delayed action of corticosteroid stress hormones on PFC glutamatergic transmission suggests a gene-mediated mechanism. GR is a ligand-inducible transcription factor. Activated GR can modify gene transcription via transactivation and transrepression.⁴⁴ In search of the downstream intracellular molecules of GRs that are potentially involved, we have found that the expression of SGK1/3 is upregulated in PFC from stressed animals, and the corticosterone-induced potentiation of NMDAR and AMPAR currents requires SGK1/3. SGK1 was originally found as an immediate early gene transcriptionally stimulated by serum and glucocorticoids.¹³ Activation of SGK1 after exposure to serum triggers entry of SGK1 into the nucleus, whereas activation of SGK1 by glucocorticoids enhances cytosolic localization of the kinase.⁴⁵ The two closely related isoforms, SGK2 and SGK3, share 80% identity in their catalytic domain with SGK1.²⁰ SGKs are widely expressed in almost all tissues, and participate in a wide variety of physiological functions, including the regulation of transport, metabolism, hormone release, cell excitability, cell proliferation, and apoptosis.⁴⁶ However, the cellular targets and functional significance of SGKs in central nervous system are far from being understood.

Studies in *Xenopus* oocytes have found that SGK plays an important role in activating certain ion channels and transporters.⁴⁶ One major mechanism underlying the action of SGK is to increase protein abundance in the plasma membrane of *Xenopus* oocytes, including epithelial sodium channels, epithelial Ca²⁺ channel TRPV5, GluR1 subunit, and KCNQ1/KCNE1 potassium channels.^{47–50} However, heterologous systems often lack the neuron-specific channel subunit composition and channel anchoring/targeting protein expression. Our results have revealed the role of SGK in stress-induced regulation of NMDAR and AMPAR trafficking in native neurons.

Emerging evidence suggests that the trafficking of AMPARs and NMDARs plays a key role in controlling excitatory synaptic efficacy.^{18,51} A key regulator for all stages of membrane traffic is Rab proteins, the largest family of monomeric small GTPases.⁵² These molecules are highly compartmentalized in organelle membranes, coordinating intracellular transport steps in exocytic and endocytic pathways, such as vesicle formation and motility, tethering/docking of vesicles to their target compartment, and interaction of vesicles with cytoskeletal elements.¹⁴ Several groups including us have found that different Rab members are involved in the internalization, recycling or spine delivery of NMDARs and AMPARs.^{53–55} The stress-induced increase in glutamatergic transmission could be due to increased exocytosis/recycling or decreased endocytosis of NMDARs and AMPARs that are controlled by different Rab members.

Cellular knockdown experiments demonstrate that the corticosterone-induced potentiation of NMDAR and AMPAR currents requires Rab4, a small GTPase that controls a direct recycling route from the early endosomes to the cell surface.²⁹ It has been shown that Rab4 is enriched on early endosomes and at least partially depleted from recycling endosomes.³⁰ Over-expressing wild-type Rab4 in cell lines decreases endocytosis and alters transferrin receptor recycling by causing its redistribution from endosomes to the plasma membrane.²⁹ Our results have revealed the role of Rab4 in stress-induced regulation of NMDAR and AMPAR trafficking in native neurons. In agreement with this, biochemical assays illustrate that Rab4 activity is selectively increased by acute stress via an SGK-dependent mechanism.

It is known that stress exerts complex influence on learning and memory processes, which is usually dependent on the action of stress hormones in combination with neuronal activities within the key target areas.⁵⁶ The PFC is an essential component of a neural circuit for working memory,¹¹ the process by which information is coded into memory, actively maintained and subsequently retrieved for guiding behavior. Delineating mechanisms by which stress affects working memory is critical for understanding the role of stress in influencing higher cognitive processes including reasoning, planning and problem solving. Acute stressful experience has been found to enhance associative learning^{57,58} in a glucocorticoid-dependent manner.⁵⁹ On the other hand, severe or chronic stress has been shown to impair working memory and prefrontal function.⁶⁰ Thus, the “inverted U” relationship of stress to cognitive function has been proposed, in which a moderate level of glucocorticoids has pro-cognitive effects, while too low or too high glucocorticoid levels are detrimental to cognitive processing.^{36,7}

Working memory is subject to the regulation by several molecules, including catecholamines and PKA.^{61,62} Alterations of these signaling molecules have been suggested to underlie prefrontal cortical impairments induced by chronic stress in mental illness.⁶³ We show that acute stress facilitates working memory in young rodents, which is correlated with the increased PFC glutamatergic transmission by acute stress.¹² Inhibiting SGK, which blocks stress-induced enhancement of glutamatergic transmission, also blocks stress-induced facilitation of working memory, suggesting that the GR/SGK-induced glutamate receptor trafficking in PFC may underlie the working memory improvement by acute stress.

Taken together, our results have discovered the molecular and cellular mechanisms underlying a form of long-term potentiation induced by acute stress (Supplemental Figure 7). These findings should provide valuable targets for designing novel therapies that modify the neuronal stress response.⁶⁴

Supplementary Material

Refer to Web version on PubMed Central for supplementary material.

Acknowledgments

We thank Dr. Rob Malenka (Stanford University) for helpful comments on the manuscript. We also thank Xiaoping Chen and Dr. Derek Daniels (Department of Psychology, SUNY at Buffalo) for excellent technical support. This work was supported by NIH grants to Z.Y.

References

1. McEwen BS. Protective and damaging effects of stress mediators. *N Engl J Med.* 1998; 338:171–9. [PubMed: 9428819]
2. McEwen BS. Stress and hippocampal plasticity. *Annu Rev Neurosci.* 1999; 22:105–22. [PubMed: 10202533]
3. McEwen BS. Physiology and neurobiology of stress and adaptation: central role of the brain. *Physiol Rev.* 2007; 87:873–904. [PubMed: 17615391]
4. Funder JW. Glucocorticoid and mineralocorticoid receptors: biology and clinical relevance. *Annu Rev Med.* 1997; 48:231–40. [PubMed: 9046958]
5. Herman JP, Figueiredo H, Mueller NK, Ulrich-Lai Y, Ostrander MM, Choi DC, Cullinan WE. Central mechanisms of stress integration: hierarchical circuitry controlling hypothalamo-pituitary-adrenocortical responsiveness. *Front Neuroendocrinol.* 2003; 24:151–80. [PubMed: 14596810]
6. de Kloet ER, Joëls M, Holsboer F. Stress and the brain: from adaptation to disease. *Nat Rev Neurosci.* 2005; 6:463–75. [PubMed: 15891777]

7. Joëls M. Corticosteroid effects in the brain: U-shape it. *Trends Pharmacol Sci.* 2006; 27:244–50. [PubMed: 16584791]
8. Lupien SJ, McEwen BS, Gunnar MR, Heim C. Effects of stress throughout the lifespan on the brain, behaviour and cognition. *Nat Rev Neurosci.* 2009; 10:434–45. [PubMed: 19401723]
9. Liston C, Miller MM, Goldwater DS, Radley JJ, Rocher AB, Hof PR, Morrison JH, McEwen BS. Stress-induced alterations in prefrontal cortical dendritic morphology predict selective impairments in perceptual attentional set-shifting. *J Neurosci.* 2006; 26:7870–4. [PubMed: 16870732]
10. Cerqueira JJ, Mailliet F, Almeida OF, Jay TM, Sousa N. The prefrontal cortex as a key target of the maladaptive response to stress. *J Neurosci.* 2007; 27:2781–7. [PubMed: 17360899]
11. Goldman-Rakic PS. Cellular basis of working memory. *Neuron.* 1995; 14:477–485. [PubMed: 7695894]
12. Yuen EY, Liu W, Karatsoreos IN, Feng J, McEwen BS, Yan Z. Acute stress enhances glutamatergic transmission in prefrontal cortex and facilitates working memory. *Proc Natl Acad Sci U S A.* 2009; 106:14075–9. [PubMed: 19666502]
13. Webster MK, Goya L, Ge Y, Maiyar AC, Firestone GL. Characterization of SGK, a novel member of the serine/threonine protein kinase gene family which is transcriptionally induced by glucocorticoids and serum. *Mol Cell Biol.* 1993; 13:2031–40. [PubMed: 8455596]
14. Zerial M, McBride H. Rab proteins as membrane organizers. *Nat Rev Mol Cell Biol.* 2001; 2:107–17. [PubMed: 11252952]
15. Yuen EY, Jiang Q, Chen P, Gu Z, Feng J, Yan Z. Serotonin 5-HT_{1A} receptors regulate NMDA receptor channels through a microtubule-dependent mechanism. *J Neurosci.* 2005; 25:5488–5501. [PubMed: 15944377]
16. Karst H, Joëls M. Corticosterone slowly enhances miniature excitatory postsynaptic current amplitude in mice CA1 hippocampal cells. *J Neurophysiol.* 2005; 94:3479–86. [PubMed: 16033944]
17. Groc L, Choquet D, Chaouloff F. The stress hormone corticosterone conditions AMPAR surface trafficking and synaptic potentiation. *Nat Neurosci.* 2008; 11:868–70. [PubMed: 18622402]
18. Malinow R, Malenka RC. AMPA receptor trafficking and synaptic plasticity. *Annu Rev Neurosci.* 2002; 25:103–26. [PubMed: 12052905]
19. Kiehl A, Bochorishvili G, Corson J, Zhang L, Rosin DL, Heggelund P, Zhu JJ. Activity patterns govern synapse-specific AMPA receptor trafficking between deliverable and synaptic pools. *Neuron.* 2009; 62:84–101. [PubMed: 19376069]
20. Kobayashi T, Cohen P. Activation of serum- and glucocorticoid-regulated protein kinase by agonists that activate phosphatidylinositol 3-kinase is mediated by 3-phosphoinositide-dependent protein kinase-1 (PDK1) and PDK2. *Biochem J.* 1999; 339:319–28. [PubMed: 10191262]
21. Lang F, Cohen P. Regulation and physiological roles of serum- and glucocorticoid-induced protein kinase isoforms. *Sci STKE.* 2001; 108:RE17. [PubMed: 11707620]
22. Schwarze SR, Ho A, Vocero-Akbani A, Dowdy SF. In vivo protein transduction: delivery of a biologically active protein into the mouse. *Science.* 1999; 285:1569–1572. [PubMed: 10477521]
23. Yang L, Dan HC, Sun M, Liu Q, Sun XM, Feldman RI, Hamilton AD, Polokoff M, Nicosia SV, Herlyn M, Sehti SM, Cheng JQ. Akt/protein kinase B signaling inhibitor-2, a selective small molecule inhibitor of Akt signaling with antitumor activity in cancer cells overexpressing Akt. *Cancer Res.* 2004; 64:4394–9. [PubMed: 15231645]
24. Zhu JJ, Qin Y, Zhao M, Van Aelst L, Malinow R. Ras and Rap control AMPA receptor trafficking during synaptic plasticity. *Cell.* 2002; 110:443–55. [PubMed: 12202034]
25. Qin Y, Zhu Y, Baumgart JP, Stornetta RL, Seidenman K, Mack V, van Aelst L, Zhu JJ. State-dependent Ras signaling and AMPA receptor trafficking. *Genes Dev.* 2005; 19:2000–15. [PubMed: 16107614]
26. Aarts M, Liu Y, Liu L, Besshoh S, Arundine M, Gurd JW, Wang YT, Salter MW, Tymianski M. Treatment of ischemic brain damage by perturbing NMDA receptor-PSD-95 protein interactions. *Science.* 2002; 298:846–50. [PubMed: 12399596]
27. Liu XJ, Gingrich JR, Vargas-Caballero M, Dong YN, Sengar A, Beggs S, Wang SH, Ding HK, Frankland PW, Salter MW. Treatment of inflammatory and neuropathic pain by uncoupling Src from the NMDA receptor complex. *Nat Med.* 2008; 14:1325–32. [PubMed: 19011637]

28. Bucci C, Parton RG, Mather IH, Stunnenberg H, Simons K, Hoflack B, Zerial M. The small GTPase rab5 functions as a regulatory factor in the early endocytic pathway. *Cell*. 1992; 70:715–28. [PubMed: 1516130]
29. van der Sluijs P, Hull M, Webster P, Mâle P, Goud B, Mellman I. The small GTP-binding protein rab4 controls an early sorting event on the endocytic pathway. *Cell*. 1992; 70:729–40. [PubMed: 1516131]
30. Sheff DR, Daro EA, Hull M, Mellman I. The receptor recycling pathway contains two distinct populations of early endosomes with different sorting functions. *J Cell Biol*. 1999; 145:123–39. [PubMed: 10189373]
31. Ullrich O, Reinsch S, Urbé S, Zerial M, Parton RG. Rab11 regulates recycling through the pericentriolar recycling endosome. *J Cell Biol*. 1996; 135:913–24. [PubMed: 8922376]
32. Vitale G, Rybin V, Christoforidis S, Thornqvist P, McCaffrey M, Stenmark H, Zerial M. Distinct Rab-binding domains mediate the interaction of Rabaptin-5 with GTP-bound Rab4 and Rab5. *EMBO J*. 1998; 17:1941–51. [PubMed: 9524117]
33. Lisman JE, Fellous JM, Wang XJ. A role for NMDA-receptor channels in working memory. *Nat Neurosci*. 1998; 1:273–5. [PubMed: 10195158]
34. Larsen JK, Divac I. Selective ablations within the prefrontal cortex of the rat and performance of delayed alternation. *Physiol Psychol*. 1978; 6:15–17.
35. Joëls M. Functional actions of corticosteroids in the hippocampus. *Eur J Pharmacol*. 2008; 583:312–21. [PubMed: 18275953]
36. Diamond DM, Bennett MC, Fleshner M, Rose GM. Inverted-U relationship between the level of peripheral corticosterone and the magnitude of hippocampal primed burst potentiation. *Hippocampus*. 1992; 2:421–430. [PubMed: 1308198]
37. Xu L, Anwyl R, Rowan MJ. Behavioural stress facilitates the induction of long-term depression in the hippocampus. *Nature*. 1997; 387:497–500. [PubMed: 9168111]
38. Xu L, Holscher C, Anwyl R, Rowan MJ. Glucocorticoid receptor and protein/RNA synthesis-dependent mechanisms underlie the control of synaptic plasticity by stress. *Proc Natl Acad Sci U S A*. 1998; 95:3204–8. [PubMed: 9501241]
39. Karst H, Berger S, Turiault M, Tronche F, Schütz G, Joëls M. Mineralocorticoid receptors are indispensable for nongenomic modulation of hippocampal glutamate transmission by corticosterone. *Proc Natl Acad Sci U S A*. 2005; 102:19204–7. [PubMed: 16361444]
40. Wiegert O, Joëls M, Krugers H. Timing is essential for rapid effects of corticosterone on synaptic potentiation in the mouse hippocampus. *Learn Mem*. 2006; 13:110–3. [PubMed: 16547165]
41. Kim JJ, Diamond DM. The stressed hippocampus, synaptic plasticity and lost memories. *Nat Rev Neurosci*. 2002; 3:453–62. [PubMed: 12042880]
42. Otani S, Blond O, Desce JM, Crepel F. Dopamine facilitates long-term depression of glutamatergic transmission in rat prefrontal cortex. *Neuroscience*. 1998; 85:669–76. [PubMed: 9639264]
43. Zhong P, Liu W, Gu Z, Yan Z. Serotonin facilitates long-term depression induction in prefrontal cortex via p38 MAPK/Rab5-mediated enhancement of AMPA receptor internalization. *J Physiol*. 2008; 586:4465–79. [PubMed: 18653660]
44. Beato M, Sánchez-Pacheco A. Interaction of steroid hormone receptors with the transcription initiation complex. *Endocr Rev*. 1996; 17:587–609. [PubMed: 8969970]
45. Firestone GL, Giampaolo JR, O'Keeffe BA. Stimulus-dependent regulation of serum and glucocorticoid inducible protein kinase (SGK) transcription, subcellular localization and enzymatic activity. *Cell Physiol Biochem*. 2003; 13:1–12. [PubMed: 12649597]
46. Lang F, Böhmer C, Palmada M, Seeböhm G, Strutz-Seeböhm N, Vallon V. (Patho)physiological significance of the serum- and glucocorticoid-inducible kinase isoforms. *Physiol Rev*. 2006; 86:1151–78. [PubMed: 17015487]
47. Alvarez de la Rosa D, Zhang P, Náray-Fejes-Tóth A, Fejes-Tóth G, Canessa CM. The serum and glucocorticoid kinase sgk increases the abundance of epithelial sodium channels in the plasma membrane of *Xenopus* oocytes. *J Biol Chem*. 1999; 274:37834–9. [PubMed: 10608847]
48. Embark HM, Setiawan I, Poppendieck S, van de Graaf SF, Boehmer C, Palmada M, Wieder T, Gerstberger R, Cohen P, Yun CC, Bindels RJ, Lang F. Regulation of the epithelial Ca²⁺ channel TRPV5 by the NHE regulating factor NHERF2 and the serum and glucocorticoid inducible kinase

- isoforms SGK1 and SGK3 expressed in *Xenopus* oocytes. *Cell Physiol Biochem*. 2004; 14:203–12. [PubMed: 15319523]
49. Strutz-Seeböhm N, Seeböhm G, Mack AF, Wagner HJ, Just L, Skutella T, Lang UE, Henke G, Striegel M, Hollmann M, Rouach N, Nicoll RA, McCormick JA, Wang J, Pearce D, Lang F. Regulation of GluR1 abundance in murine hippocampal neurons by serum- and glucocorticoid-inducible kinase 3. *J Physiol*. 2005; 565:381–90. [PubMed: 15774536]
 50. Seeböhm G, Strutz-Seeböhm N, Birkin R, Dell G, Bucci C, Spinoso MR, Baltaev R, Mack AF, Korniyuchuk G, Choudhury A, Marks D, Pagano RE, Attali B, Pfeufer A, Kass RS, Sanguinetti MC, Tavaré JM, Lang F. Regulation of endocytic recycling of KCNQ1/KCNE1 potassium channels. *Circ Res*. 2007; 100:686–92. [PubMed: 17293474]
 51. Wenthold RJ, Prybylowski K, Standley S, Sans N, Petralia RS. Trafficking of NMDA receptors. *Annu Rev Pharmacol Toxicol*. 2003; 43:335–58. [PubMed: 12540744]
 52. Pfeffer SR. Rab GTPases: specifying and deciphering organelle identity and function. *Trends Cell Biol*. 2001; 11:487–91. [PubMed: 11719054]
 53. Brown TC, Tran IC, Backos DS, Esteban JA. NMDA receptor-dependent activation of the small GTPase Rab5 drives the removal of synaptic AMPA receptors during hippocampal LTD. *Neuron*. 2005; 45:81–94. [PubMed: 15629704]
 54. Park M, Penick EC, Edwards JG, Kauer JA, Ehlers MD. Recycling endosomes supply AMPA receptors for LTP. *Science*. 2004; 305:1972–5. [PubMed: 15448273]
 55. Chen P, Gu Z, Liu W, Yan Z. Glycogen synthase kinase 3 regulates NMDA receptor channel trafficking and function in cortical neurons. *Mol Pharmacol*. 2007; 72:40–51. [PubMed: 17400762]
 56. Shors TJ. Stressful experience and learning across the lifespan. *Annu Rev Psychol*. 2006; 57:55–85. [PubMed: 16318589]
 57. Shors TJ, Weiss C, Thompson RF. Stress-induced facilitation of classical conditioning. *Science*. 1992; 257:537–9. [PubMed: 1636089]
 58. Joëls M, Pu Z, Wiegert O, Oitzl MS, Krugers HJ. Learning under stress: how does it work? *Trends Cogn Sci*. 2006; 10:152–8. [PubMed: 16513410]
 59. Beylin AV, Shors TJ. Glucocorticoids are necessary for enhancing the acquisition of associative memories after acute stressful experience. *Horm Behav*. 2003; 43:124–31. [PubMed: 12614642]
 60. Arnsten AF. Stress signalling pathways that impair prefrontal cortex structure and function. *Nat Rev Neurosci*. 2009; 10:410–22. [PubMed: 19455173]
 61. Vijayraghavan S, Wang M, Birnbaum SG, Williams GV, Arnsten AF. Inverted-U dopamine D1 receptor actions on prefrontal neurons engaged in working memory. *Nat Neurosci*. 2007; 10:376–84. [PubMed: 17277774]
 62. Wang M, et al. Alpha2A-adrenoceptors strengthen working memory networks by inhibiting cAMP-HCN channel signaling in prefrontal cortex. *Cell*. 2007; 129:397–410. [PubMed: 17448997]
 63. Hains AB, Arnsten AF. Molecular mechanisms of stress-induced prefrontal cortical impairment: implications for mental illness. *Learn Mem*. 2008; 15:551–64. [PubMed: 18685145]
 64. Kaufer D, Ogle WO, Pincus ZS, Clark KL, Nicholas AC, Dinkel KM, Dumas TC, Ferguson D, Lee AL, Winters MA, Sapolsky RM. Restructuring the neuronal stress response with anti-glucocorticoid gene delivery. *Nat Neurosci*. 2004; 7:947–53. [PubMed: 15300253]

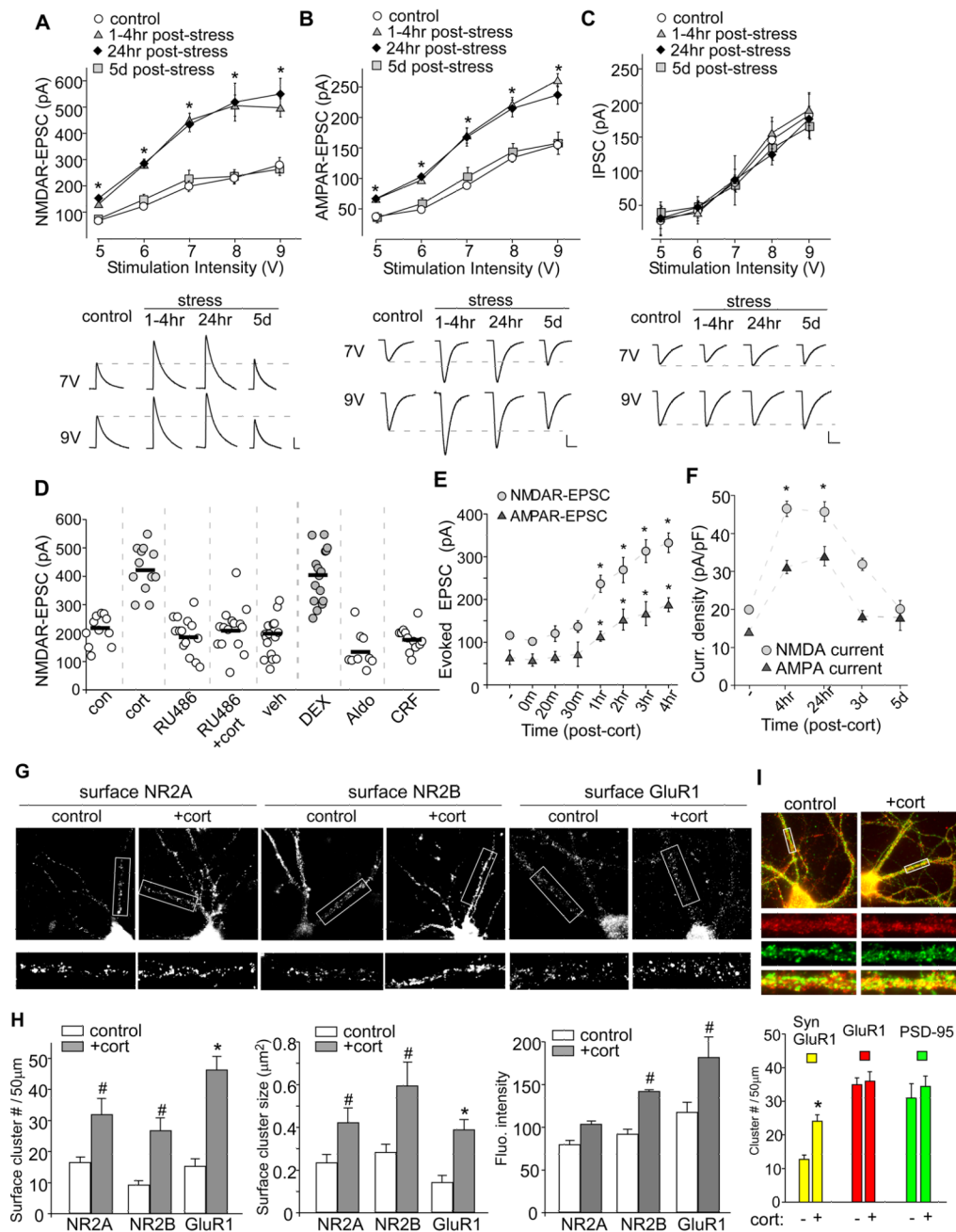


Figure 1. Acute stress or *in vitro* corticosterone treatment enhances the synaptic response and surface expression of NMDARs and AMPARs in PFC pyramidal neurons via activation of GRs
A–C, Summarized input-output curves of NMDAR-EPSC (A), AMPAR-EPSC (B) or GABA_A-IPSC (C) evoked by a series of stimulus intensities in PFC pyramidal neurons taken from control or animals exposed to forced-swim stress (examined at 1–4 hr, 24 hr and 5 days post-stress). Inset: Representative synaptic current traces. Scale bars: 100 pA, 100 ms (A); 50 pA, 20 ms (B); 50 pA, 40 ms (C). *: $p < 0.001$. **D**, Dot plot showing the amplitude of NMDAR-EPSC in PFC neurons treated without or with corticosterone (cort, 100 nM, 20 min), RU486 (20 μM, 20 min), RU486+cort, vehicle (DMSO, 20 min), dexamethasone (DEX, 100 nM, 20 min), aldosterone (Aldo, 10 nM, 20 min) or corticotrophin releasing factor (CRF, 200 nM, 20 min). Recordings were obtained 1–4 hr after the treatment. **E,F**,

Plots of NMDAR-EPSC and AMPAR-EPSC amplitude recorded in PFC slices (E) or NMDAR and AMPAR current density recorded in PFC cultures (F) at various time points post-corticosterone treatment (100 nM, 20 min). **G**, Immunocytochemical images of surface GFP-NR2A (A), GFP-NR2B (B) and GluR1 (C) in PFC cultures treated without (control) or with corticosterone (100 nM, 20 min). Enlarged versions of the boxed regions of dendrites are shown beneath each of the images. **H**, Quantitative analysis of surface NR2A, NR2B and GluR1 clusters (cluster density, cluster size and cluster intensity) along dendrites in control vs. corticosterone-treated PFC cultures. #: $p < 0.05$, *: $p < 0.001$. **I**, Immunocytochemical images (upper panel) and quantitative analysis (lower panel) of synaptic GluR1 (PSD-95 co-localized, yellow puncta), total GluR1 clusters (red puncta) and PSD-95 clusters (green puncta) along dendrites in control vs. corticosterone (100 nM, 20 min)-treated PFC cultures. Enlarged versions of the boxed regions of dendrites are also shown. *: $p < 0.001$.

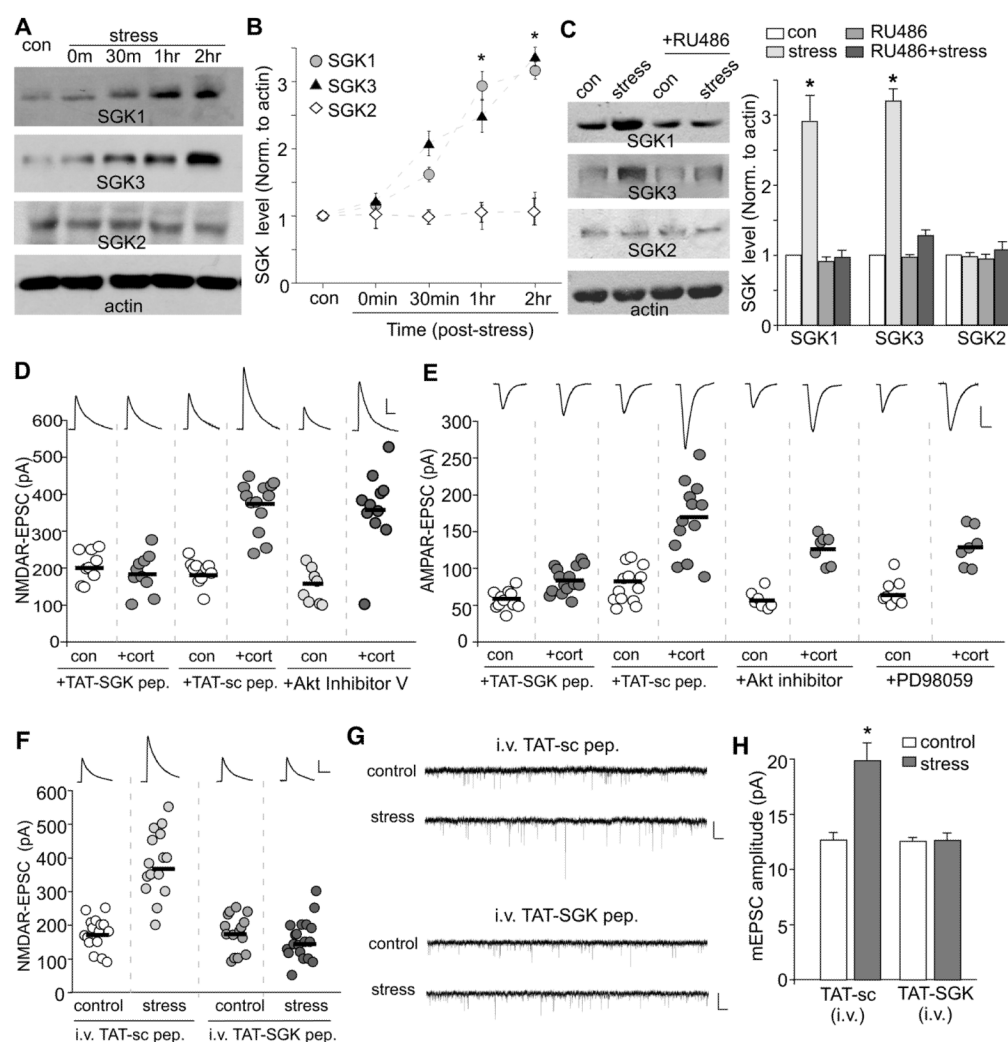


Figure 2. SGK is upregulated in PFC by acute stress via GR and is necessary for acute stress-induced potentiation of glutamatergic transmission

A,B, Western blots (A) and quantification (B) of SGKs in lysates of PFC slices taken from control or stressed animals at various post-stress time points (0 min, 30 min, 1 hr and 2 hr). *: $p < 0.001$. **C**, Western blots and quantification of SGKs in lysates of PFC slices taken from control or stressed animals without or with i.p. injection of RU486 (10 mg/kg, administered 30 min before stress). Blotting was done 1 hr post-stress. *: $p < 0.001$. **D,E**, Dot plots of NMDAR-EPSC (D) or AMPAR-EPSC (E) recorded in PFC slices treated with or without corticosterone (100 nM, 20 min) in the presence of TAT-SGK peptide (1 μM), scrambled peptide (TAT-sc, 1 μM), Akt Inhibitor V (20 μM) or p42/44 MAPK kinase inhibitor PD98059 (40 μM). Peptides or compounds were added 30 min prior to corticosterone. Recordings were performed at 1–4 hrs after corticosterone treatment. **F**, Dot plots of NMDAR-EPSC recorded in PFC slices from control vs. stressed animals i.v. injected with TAT-SGK peptide (0.6 pmol/g) or a scrambled control peptide (TAT-sc, 0.6 pmol/g). Peptides were administered 30 min prior to stress, and recordings were performed at 1–4 hrs post-stress. Inset (D–F): Representative NMDAR-EPSC or AMPAR-EPSC traces. Scale bars: 100 pA, 100 ms (NMDA); 50 pA, 20 ms (AMPA). **G,H**, Representative mEPSC traces (G) and bar graphs of mEPSC amplitude (mean ± SEM, H) in PFC slices from control vs. stressed animals i.v. injected with different peptides. Scale bars (G): 10 pA, 1 s. *: $p < 0.001$.

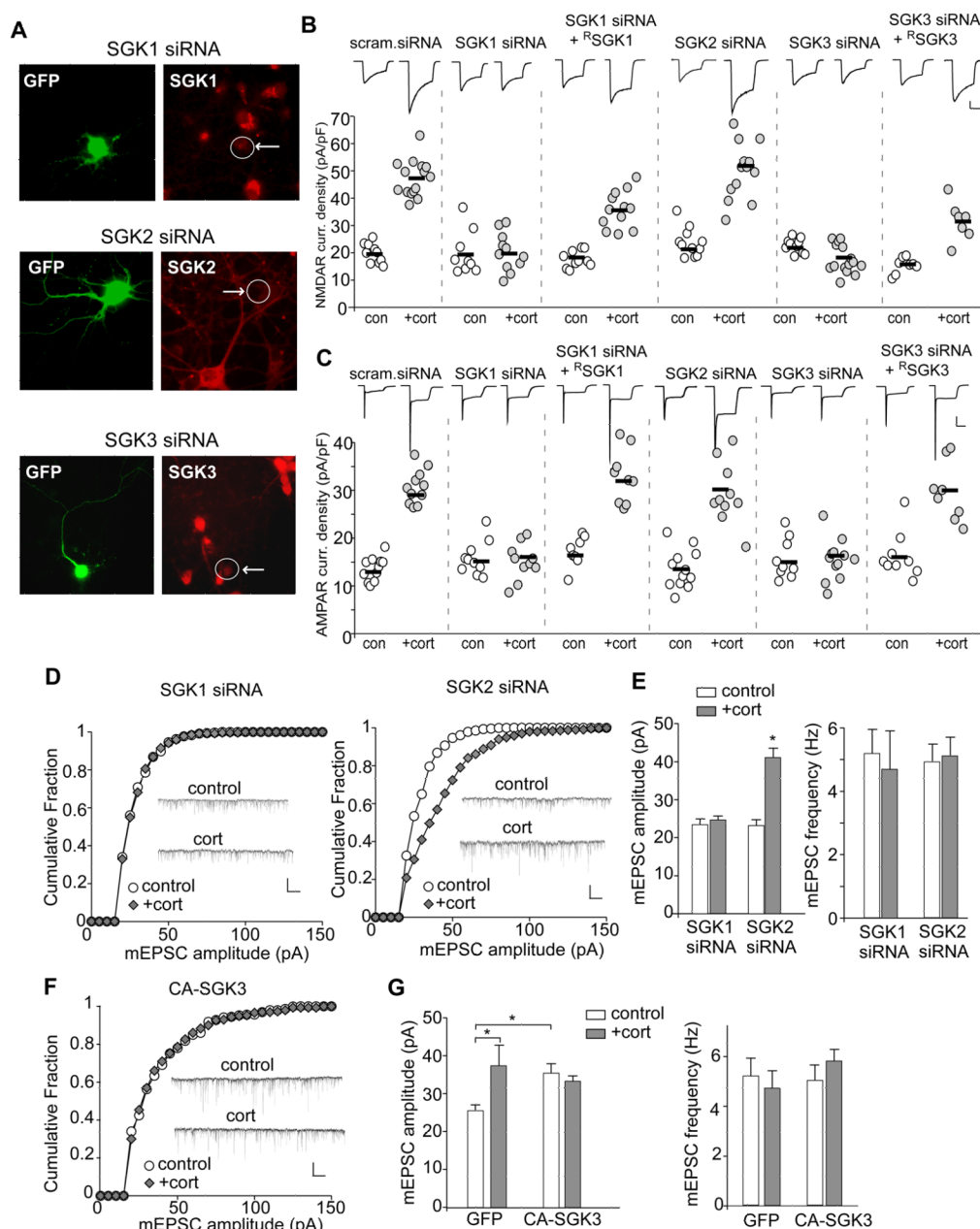


Figure 3. SGK1 and SGK3 are involved in corticosterone enhancement of NMDAR and AMPAR currents

A, Immunocytochemical staining of SGK1, SGK2, or SGK3 in cultured PFC neurons transfected with siRNA against each SGK isoform. GFP was co-transfected to illuminate positive neurons. **B,C**, Dot plots showing the effect of corticosterone treatment (100 nM, 20 min) on NMDAR (**B**) or AMPAR (**C**) current density in PFC cultures transfected with a scrambled siRNA or siRNA against each SGK isoform. The siRNA-resistant silent mutant of SGK1 (^RSGK1) or SGK3 (^RSGK3) was co-transfected in the rescue experiments. Recordings were obtained 1–4 hr after the treatment. Inset: Representative current traces. Scale bars: 200 pA, 1 sec. **D,F**, Cumulative distribution of mEPSC amplitude in PFC cultures (DIV21) transfected with SGK1 siRNA or SGK2 siRNA (**D**), or constitutively activating SGK3 (CA-SGK3, **F**). Two or three days after transfection, neurons were treated

with or without corticosterone (100 nM) for 20 min, and recorded 24 hr later. Inset: Representative mEPSC traces. Scale bar: 50 pA, 1 sec. **E,G**, Bar graphs (mean \pm SEM) showing the mEPSC amplitude and frequency with corticosterone treatment in neurons transfected with different siRNAs (E) or constructs (G). *: $p < 0.01$.

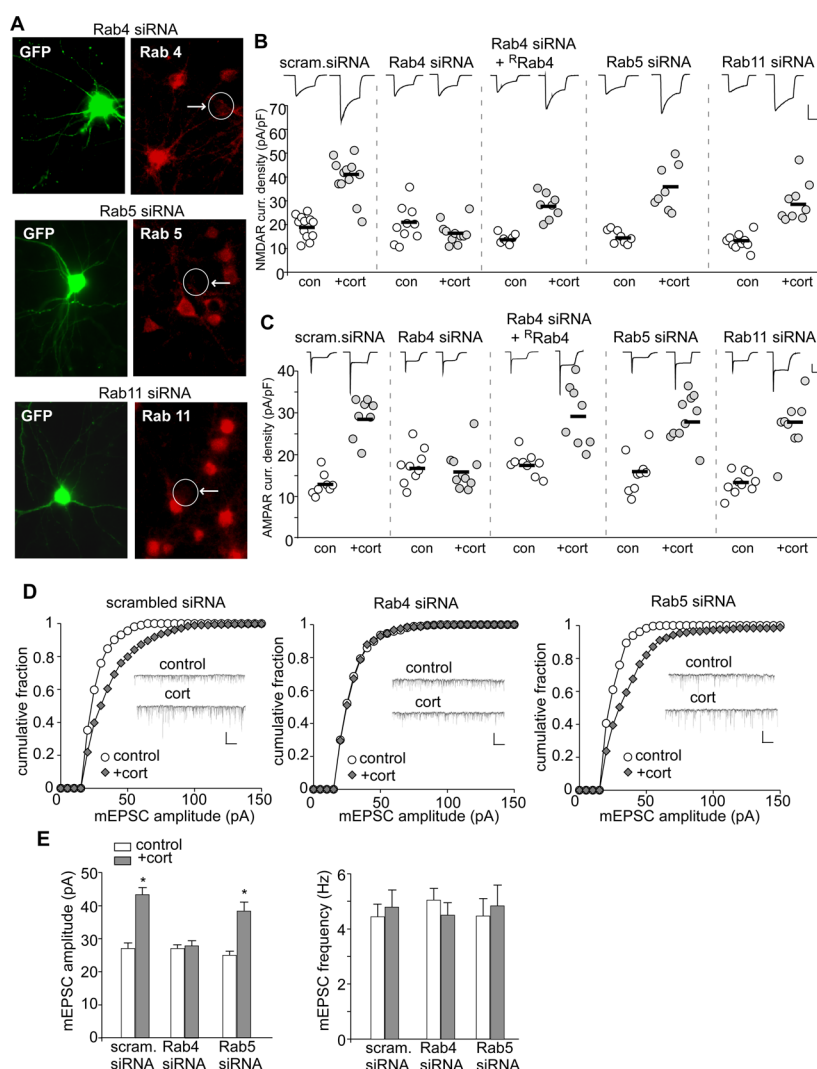


Figure 4. Corticosterone increases NMDAR and AMPAR currents via a Rab4-dependent mechanism

A, Immunocytochemical staining of Rab4, Rab5 or Rab11 in cultured PFC neurons transfected with siRNA against each Rab member. GFP was co-transfected to illuminate positive neurons. **B,C**, Dot plots showing the effect of corticosterone treatment (100 nM, 20 min) on NMDAR (B) or AMPAR (C) current density in PFC cultures transfected with a scrambled siRNA or siRNA against Rab4, Rab5 or Rab11. The siRNA-resistant silent mutant of Rab4 (^RRab4) was co-transfected in the rescue experiments. Recordings were obtained 1–4 hr after the treatment. Inset: Representative current traces. Scale bars: 200 pA, 1 sec. **D**, Cumulative distribution of mEPSC amplitude in PFC cultures (DIV21) transfected with a scrambled siRNA, Rab4 siRNA, or Rab5 siRNA. Two or three days after transfection, neurons were treated with or without corticosterone (100 nM) for 20 min, and recorded 24 hr later. Inset: Representative mEPSC traces. Scale bar: 50 pA, 1 sec. **E**, Bar graphs (mean ± SEM) showing the mEPSC amplitude and frequency with corticosterone treatment in neurons transfected with different siRNAs. *: p<0.001.

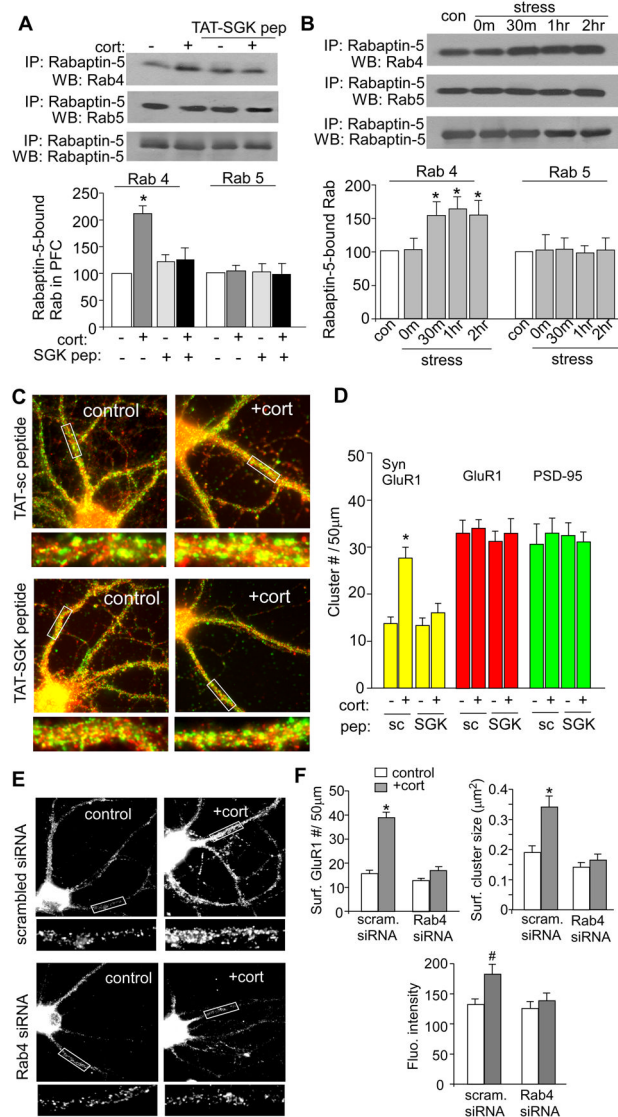


Figure 5. Corticosterone activates Rab4 through a SGK-dependent mechanism, and SGK inhibition or Rab4 knockdown blocks the enhancing effect of corticosterone on glutamate receptor trafficking

A,B, Top panel: Co-immunoprecipitation blots showing the level of active (Rabaptin-5-bound) Rab4 or Rab5 in PFC slices without or with corticosterone treatment (100 nM, 20 min, collected 1 hr after treatment) in the absence or presence of TAT-SGK peptide (50 µM, 30 min prior to corticosterone, A), or in PFC slices from control vs. swim-stressed animals examined at various post-stress time points (B). Lower panel: Quantification showing the normalized level of Rabaptin-5-bound (active) Rab4 or Rab5 in PFC slices without vs. with corticosterone treatment (A) or from control vs. stressed animals (B). *: $p < 0.001$. **C,D**, Immunocytochemical images (C) and quantitative analysis (D) of synaptic GluR1 clusters (PSD-95 co-localized, yellow puncta), total GluR1 clusters (red puncta) and PSD-95 clusters (green puncta) in control vs. corticosterone (100 nM, 20 min)-treated PFC pyramidal neurons from cultures pre-treated with TAT-SGK peptide (50 µM) or the scrambled control peptide (TAT-sc). Enlarged versions of the boxed dendritic regions are also shown. *: $p < 0.001$. **E**, Immunocytochemical images of surface GluR1 in cultured PFC neurons

(DIV21–23) transfected with a scrambled siRNA or Rab4 siRNA. Two or three days after transfection, neurons were treated with or without corticosterone (100 nM) for 20 min, and stained 24 hrs later. **F**, Quantitative analysis of surface GluR1 clusters along dendrites in control vs. corticosterone-treated PFC cultures with different transfections. #: $p < 0.05$, *: $p < 0.001$.

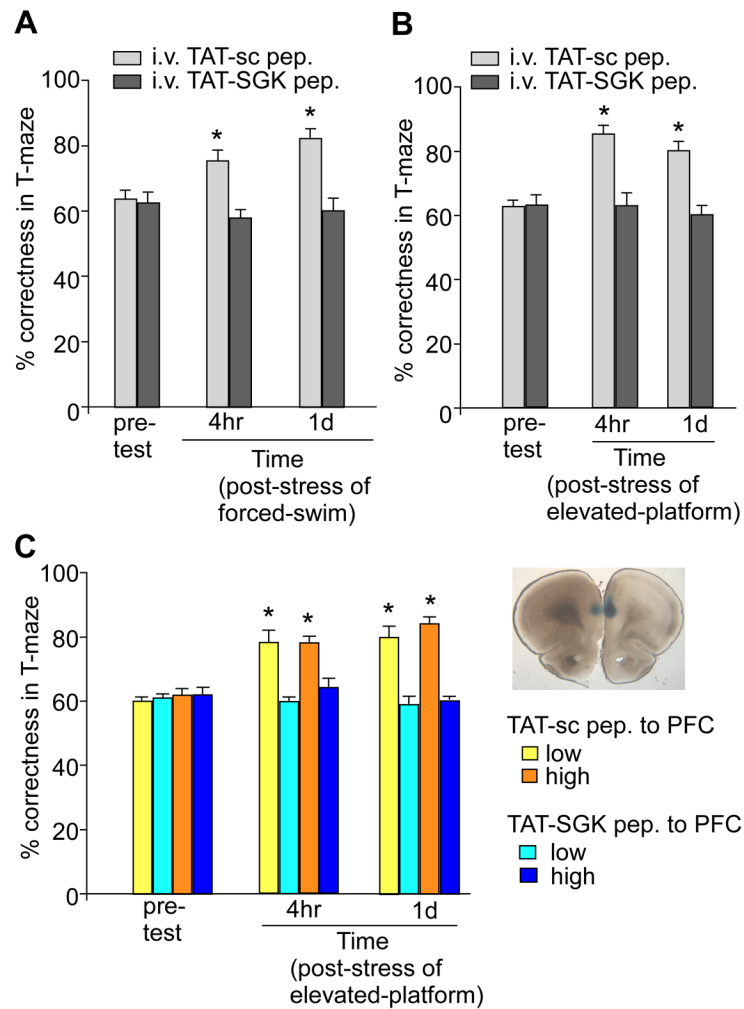


Figure 6. Acute behavioral stress enhances working memory via a SGK-dependent mechanism
A,B, Cumulative data (mean \pm SEM) showing the percentage correctness in T-maze tests before and after forced-swim stress (A) or elevated platform stress (B) in rats i.v. injected with TAT-SGK peptide vs. scrambled TAT-sc peptide (0.6 pmol/g). *: $p < 0.01$. **C,** Cumulative data (mean \pm SEM) showing the percentage correctness in T-maze tests before and after elevated platform stress in rats locally injected to PFC with TAT-SGK peptide vs. scrambled TAT-sc peptide (high dose: 40 pmol/g; low dose: 0.12 pmol/g). Inset: A photograph showing the slice with a local injection of ink to PFC prelimbic regions to confirm the appropriate location of the cannula. *: $p < 0.01$.